A Deformable Surface-Spine Model for 3-D Surface Registration

Jianhua Xuan [†‡], Yue Wang [♮‡], Tülay Adalı [†], Qinfen Zheng [♯],
Wendelin Hayes[‡], Matthew T. Freedman [‡], and Seong K. Mun [‡]

[†] Department of Computer Science and Electrical Engineering,
University of Maryland Baltimore County, Baltimore, MD 21250

[‡] ISIS Center, Department of Radiology, Georgetown University Medical Center, Washington, DC 20007

[♮] Department of Electrical Engineering, The Catholic University of America, Washington, DC 20064

[♯] Center for Automation Research, University of Maryland College Park, College Park, MD 20742

Abstract

A finite-element deformable surface-spine model is developed in this paper to register two surfaces by recovering the nonlinear deformation with respect to each other. The deformable surface-spine model is a dynamic model governed by Lagrangian motion equations. A 9 degree-of-freedom (dof) finite-element surface element and a 4-dof spine element are developed to iteratively solve Lagrangian equations for computing the deformation between two surfaces. The method has been applied to registration of computerized surgical prostate models. Experimental results have demonstrated that the new registration method can successfully match complex-structured surfaces by recovering the nonlinear deformation.

1 Introduction

Registration of three-dimensional (3-D) images is a prerequisite to fuse the complementary information available in multi-modality imagery, to study the pathological evolution of the same patient at different times, to compare the subtle changes among different patients, and to discover the statistical information of disease patterns in multi-patient cases [1]. It is well recognized that registration by geometric features has advantages over intensity-based registration methods since geometric features, such as contours, edges, and surfaces, are often presented in consistency among the multi-modality images while intensity values may not. A 3-D elastic matching algorithm has been developed in [3] for registering two surfaces based on Burr's original work on two-dimensional (2-D) contours. In this paper, we present a new 3-D registration method by using a deformable surface-spine model to match two surfaces. The deformable surface-spine model can respond dynamically to applied forces according to physical principles as partial differential equations in continuum mechanics. The dynamic property of the deformable model makes it suitable and effective to recover the non-rigid deformation between two surfaces for 3-D registration. In this paper, it is assumed that a coarse registration has been implemented by the principle axis method prior to the proposed deformable registration method. That is, our registration method is particularly developed to register those surfaces with similar size and orientation by recovering the local deformation. Section 2 describes the deformable surface-spine model and the registration method in detail. Section 3 gives experimental results and Section 4 concludes this paper.

2 Methods

A deformable surface-spine model can be described intuitively as the following coupled dynamic system [4]: The initial spine is the axis of the surface determined from its contours, then all the surface patches are contracted to the spine through expansion/compression forces radiating from the spine while the spine itself is also confined to the surfaces, as shown in Fig. 1. The dynamics of the deformable surface-spine model is governed by the second-order partial differential equations from Lagrangian mechanics, and the final shapes and relationship of the surface and spine are achieved when the energy of this dynamic deformable surface-spine model reaches its minimum.

A deformable surface-spine model can be presented in both variational and finite-element forms. First of all, we give mathematical notations for both surface and spine. The surface can be defined as $\mathbf{x}(u,v,t) = (x(u,v,t), y(u,v,t), z(u,v,t))$, where $(u,v) \in [0,1]^2$ are the bivariate material coordinates, $x(u,v,t), y(u,v,t)$, and $z(u,v,t)$ are the coordinates of a point on the surface in $\Re^3$; t denotes the time-varying property of the deformable surface. Similarly, the spine can be defined as $\mathbf{x}(s,t) = (x(s,t), y(s,t), z(s,t))$, where $s \in [0,1]$ is the univariate material coordinate and $x(s,t), y(s,t)$, and $z(s,t)$ are the coordinates of a point on the spine in $\Re^3$.

The strain energy $\mathcal{E}$ can be found to characterize the deformable material of either the surface or spine, which will be discussed in the next section as an instance of the spline function. Then the continuum mechanical equation

$$\mu \frac{\partial^2 \mathbf{x}}{\partial t^2} + \gamma \frac{\partial \mathbf{x}}{\partial t} + \frac{\delta \mathcal{E}(\mathbf{x})}{\delta \mathbf{x}} = \mathbf{f}(\mathbf{x}), \qquad (1)$$

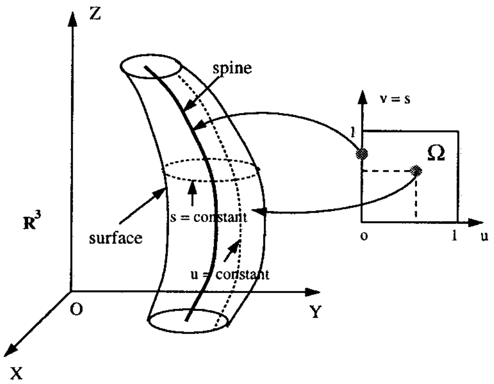

Figure 1: The deformable surface-spine model.

governs the non-rigid motion of the surface (spine) in response to an extrinsic force $\mathbf{f}(\mathbf{x})$, where μ is the mass density function of the deformable surface (spine) and γ is the viscosity function of the ambient medium. The third term on the left-hand side of the equation is the variational derivative of the strain energy functional $\mathcal{E}$, the internal elastic force of the surface (spine).

2.1 Variational Modeling

The deformable energy of surface $\mathbf{x}(u, v, t)$ can be defined by

$$\mathcal{E}_{surface}(u,v,t) = \int_0^1 \int_0^1 \left(w_{10} \left| \frac{\partial \mathbf{x}}{\partial u} \right|^2 + 2w_{11} \left| \frac{\partial \mathbf{x}}{\partial u} \right| \left| \frac{\partial \mathbf{x}}{\partial v} \right| + w_{01} \left| \frac{\partial \mathbf{x}}{\partial v} \right|^2 + w_{20} \left| \frac{\partial^2 \mathbf{x}}{\partial u^2} \right|^2 + 2w_{22} \left| \frac{\partial^2 \mathbf{x}}{\partial u \partial v} \right|^2 + w_{02} \left| \frac{\partial^2 \mathbf{x}}{\partial v^2} \right|^2 \right) du dv, \quad (2)$$

where the weights w_{10}, w_{11} and w_{01} control the tensions of the surface, while w_{20}, w_{22} and w_{02} control its rigidities (bending energy). The deformable energy of spine $\mathbf{x}(s, t)$ is given by

$$\mathcal{E}_{spine}(s,t) = \int_0^1 \left(w_1 \left| \frac{d\mathbf{x}}{ds} \right|^2 + w_2 \left| \frac{d^2\mathbf{x}}{ds^2} \right|^2 \right) ds. \quad (3)$$

The weight w_1 controls the tension along the spine (stretching energy), while w_2 controls its rigidity (bending energy).

To couple the surface with the spine, we enforce $v \equiv s$, which maps the spine coordinate into the coordinate along the length of the surface as shown in Fig. 1. Then we connect the spine with surface by introducing following forces on the surface and spine respectively [4]:

$$\begin{aligned} \mathbf{f}^a_{surface}(u,s,t) &= -(a/l)(\bar{\mathbf{x}}_{surface} - \mathbf{x}_{spine}) \\ \mathbf{f}^a_{spine}(s,t) &= a\ (\bar{\mathbf{x}}_{surface} - \mathbf{x}_{spine}) \quad (4) \end{aligned}$$

where a controls the strength of the forces; $\bar{\mathbf{x}}_{surface}$ is the centroid of the coordinate curve (s = constant) circling the surface and is defined as: $\bar{\mathbf{x}}_{surface} = \frac{1}{l}\int_0^1 \mathbf{x}_{surface} \left| \frac{\partial \mathbf{x}_{surface}}{\partial u} \right| du$, and l is the length of the curve (s = constant). In general, the above forces coerce the spine staying on an axial position of the surface. Further, if necessary, we can encourage the surface to be radially symmetric around the spine by introducing the following force:

$$\mathbf{f}^b_{surface} = b(\bar{\mathbf{r}} - |\mathbf{r}|)\hat{\mathbf{r}}, \quad (5)$$

where b controls the strength of the force; $\mathbf{r}$ is the radial vector of the surface with respect to the spine as $\mathbf{r}(u, s) = \mathbf{x}_{surface} - \mathbf{x}_{spine}$, the unit radial vector is $\hat{\mathbf{r}}(u, s) = \mathbf{r}/|\mathbf{r}|$, and $\bar{\mathbf{r}}(s) = \frac{1}{l}\int_0^1 |\mathbf{r}| \frac{\partial \mathbf{x}_{surface}}{\partial u} du$ is the mean radius of the coordinate curve s = constant. Also, it is possible to provide control over expansion and contraction of the surface around the spine. This can be realized by introducing the following force:

$$\mathbf{f}^c_{surface} = c\hat{\mathbf{r}}, \quad (6)$$

where c controls the strength of the expansion or contraction force. The surface will inflate where $c > 0$ and deflate where $c < 0$.

Summing the above coupling forces in the motion equation associated with surface and spine, we obtain the following dynamic system describing the motion of the deformable surface-spine model:

$$\begin{aligned} \mu \frac{\partial^2 \mathbf{x}_{\text{surface}}}{\partial t^2} + \gamma \frac{\partial \mathbf{x}_{\text{surface}}}{\partial t} + \frac{\delta \mathcal{E}_{\text{surface}}}{\delta \mathbf{x}} &= \mathbf{f}^{\text{total}}_{\text{surface}}, \\ \mu \frac{\partial^2 \mathbf{x}_{\text{spine}}}{\partial t^2} + \gamma \frac{\partial \mathbf{x}_{\text{spine}}}{\partial t} + \frac{\delta \mathcal{E}_{\text{spine}}}{\delta \mathbf{x}} &= \mathbf{f}^{\text{total}}_{\text{spine}}, \quad (7) \end{aligned}$$

where $\mathbf{f}^{total}_{surface} = \mathbf{f}^{ext}_{surface} + \mathbf{f}^a_{surface} + \mathbf{f}^b_{surface} + \mathbf{f}^c_{surface}$ and $\mathbf{f}^{total}_{spine} = \mathbf{f}^{ext}_{spine} + \mathbf{f}^a_{spine}$. Note that $\mathbf{f}^{ext}_{surface}$ is the external force applied on the surface and $\mathbf{f}^{ext}_{spine}$ the external force applied on the spine (we assign $\mathbf{f}^{ext}_{spine} = 0$ in our implementation). In surface registration problem, we are interested in matching two surfaces by computing the deformation between them. We define the external forces to reflect the distance between the two surfaces under consideration:

$$\mathbf{f}^{ext}_{surface} = C(\mathbf{x}_{surface}(u, v)), \quad (8)$$

where $C(\mathbf{x}_{surface}(u, v))$ is the Euclidean distance of each point on the first surface to the nearest point on the second surface. The final $\mathbf{x}_{surface}$ and $\mathbf{x}_{spine}$ are obtained when the energy of the deformable surface-spine reaches its minimum. To solve equation (7) of such a dynamic system, we will introduce the finite-element method in the next section.

2.2 Finite-Element Modeling

Both the finite difference method and the finite element method can be used to compute the numerical solution to the surface $\mathbf{x}_{surface}$ and spine $\mathbf{x}_{spine}$. Finite difference method approximates the continuous function $\mathbf{x}$ as a set of discrete nodes in space. A disadvantage of the finite difference approach is that the continuity of the solution between nodes is not made explicitly. The finite element method, on the other hand, provides continuous surface (or spine) approximation by representing the unknown function $\mathbf{x}$ in terms of combinations of the basis functions. In finite element method, we first tessellate the continuous material domain, (u, v) for the surface and s for the spine in our case, into a mesh of m element subdomains D_j, we then approximate $\mathbf{x}$ as a weighted sum of continuous basis functions $\mathbf{N}_i$ (so-called shape functions):

$$\mathbf{x} \approx \mathbf{x}^h = \sum_{i=1}^{n} \mathbf{x}_i \mathbf{N}_i = \mathbf{N}\ \mathbf{a}, \qquad (9)$$

where $\mathbf{x}_i$ is a vector of nodal variables associated with mesh node i, $\mathbf{N}_i$ is a vector of shape functions associated with node i, n is the number of nodes of an element, $\mathbf{a}^T = [\mathbf{x}_1^T, \cdots, \mathbf{x}_n^T]$, and $\mathbf{N} = [\mathbf{N}_1, \cdots, \mathbf{N}_n]$. The shape functions $\mathbf{N}_i$ are fixed in advance and the nodal variables $\mathbf{x}_i$ are the unknowns. The motion equation in 1 can then be discretized as

$$\mathbf{M}\frac{\partial^2 \mathbf{a}}{\partial t^2} + \mathbf{C}\frac{\partial \mathbf{a}}{\partial t} + \mathbf{K}\mathbf{a} = \mathbf{F}, \qquad (10)$$

where $\mathbf{M}$ is the mass matrix, $\mathbf{C}$ is the damping matrix, $\mathbf{K}$ is the stiffness matrix, and $\mathbf{F}$ is the forcing matrix. $\mathbf{M}$, $\mathbf{C}$, and $\mathbf{F}$ can be obtained as follows:

$$\begin{aligned} \mathbf{M} &= \int\int \mu \mathbf{N}^T \mathbf{N}\ dudv, \\ \mathbf{C} &= \int\int \gamma \mathbf{N}^T \mathbf{N}\ dudv, \qquad (11) \\ \mathbf{F} &= \int\int \mathbf{N}^T \mathbf{f}\ dudv. \end{aligned}$$

To compute $\mathbf{K}$, we have the following equation:

$$\mathbf{K} = \int\int \left(\mathbf{N}_s^T \alpha \mathbf{N}_s + \mathbf{N}_b^T \beta \mathbf{N}_b \right)\ dudv, \qquad (12)$$

where

$$\begin{aligned} \mathbf{N}_s &= \left[\frac{\partial \mathbf{N}}{\partial u}, \ \frac{\partial \mathbf{N}}{\partial v} \right]^T, \\ \mathbf{N}_b &= \left[\frac{\partial^2 \mathbf{N}}{\partial u^2}, \ 2\frac{\partial^2 \mathbf{N}}{\partial u \partial v}, \ \frac{\partial^2 \mathbf{N}}{\partial v^2} \right]^T, \qquad (13) \\ \alpha &= \begin{bmatrix} w_{10} & w_{11} \\ w_{11} & w_{01} \end{bmatrix}, \end{aligned}$$

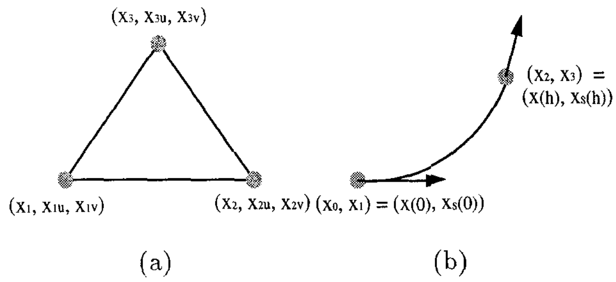

Figure 2: (a) 3-node, 9-dof triangular element, (b) 2-node, 4-dof spine element.

$$\beta = \begin{bmatrix} w_{20} & 0 & 0 \\ 0 & w_{22} & 0 \\ 0 & 0 & w_{02} \end{bmatrix}. \qquad (14)$$

2.2.1 Deformable Surface Element

The deformable surface consists of a set of connected triangular elements chosen to model a large range of topological shapes. Barycentric coordinates in two dimensions are the natural choice for defining shape functions over a triangular domain, since a unifying representation of different triangles can be achieved in Barycentric coordinates [2]. Barycentric coordinates (L_1, L_2, L_3) are defined by the following mapping with material coordinates (u, v):

$$\begin{bmatrix} u \\ v \\ 1 \end{bmatrix} = \begin{bmatrix} u_1 & u_2 & u_3 \\ v_1 & v_2 & v_3 \\ 1 & 1 & 1 \end{bmatrix} \begin{bmatrix} L_1 \\ L_2 \\ L_3 \end{bmatrix}, \qquad (15)$$

where $(u_1, v_1), (u_2, v_2)$, and (u_3, v_3) are the coordinates of three vertex locations of the triangle.

We use a 9-dof triangular element with its position and first parametric partial derivatives at each triangle vertex shown in Fig. 2(a). The shape functions for the 9-dof triangle are [5]:

$$\mathbf{N}_1^{9T} = \begin{bmatrix} L_1 + L_1^2 L_2 + L_1^2 L_3 - L_1 L_2^2 - L_1 L_3^2 \\ c_3(L_1^2 L_2 + 0.5 L_1 L_2 L_3) - c_2(L_1^2 L_3 + 0.5 L_1 L_2 L_3) \\ -b_3(L_1^2 L_2 + 0.5 L_1 L_2 L_3) + b_2(L_1^2 L_3 + 0.5 L_1 L_2 L_3) \end{bmatrix}.$$

The triangle's symmetry in Barycentric coordinates can be used to generate the shape function for the second and third nodes in terms of the first. To generate $\mathbf{N}_2^9$ use the above equations but add a 1 to each index so that $1 \rightarrow 2$, $2 \rightarrow 3$ and $3 \rightarrow 1$. The $\mathbf{N}_3^9$ functions are generated by adding another 1 to each index. By defining 9 dofs of the triangular element as

$$\mathbf{a}^T = [\mathbf{x}_1, \mathbf{x}_{1u}, \mathbf{x}_{1v}, \mathbf{x}_2, \mathbf{x}_{2u}, \mathbf{x}_{2v}, \mathbf{x}_3, \mathbf{x}_{3u}, \mathbf{x}_{3v}], \qquad (16)$$

we can approximate the $\mathbf{x}$ as

$$\mathbf{x}^h = \mathbf{N}^9\ \mathbf{a} = [\mathbf{N}_1^9\ \ \mathbf{N}_2^9\ \ \mathbf{N}_3^9]\ \mathbf{a}. \qquad (17)$$

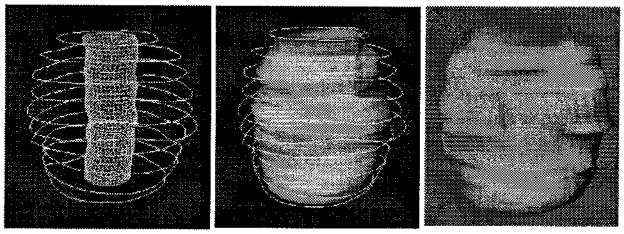

(a) (b) (c)

Figure 3: Dynamics of the deformable surface-spine model: (a) initial, (b) after 5 iterations, (c) final.

2.2.2 Deformable Spine Element

The finite element of the spine has 4 dofs between two nodes located at the ends of the segment shown in Fig. 2(b). The dofs at each node correspond to its position and tangent. The spine segment can be approximated as the weighted sum of a set of Hermite polynomials:

$$\mathbf{x} \approx \mathbf{x}^h(s) = \sum_{i=0}^{3} \mathbf{x}_i N_i, \tag{18}$$

where $\mathbf{x}_i, i = 0, \cdots, 3$ are nodal variables and $N_i, i = 0, \cdots, 3$ are given as follows:

$$\begin{aligned} N_0 &= 1 - 3(s/h)^2 + 2(s/h)^3, \\ N_1 &= h(s/h - 2(s/h)^2 + (s/h)^3), \\ N_2 &= 3(s/h)^2 - 2(s/h)^3, \\ N_3 &= h(-(s/h)^2 + (s/h)^3), \end{aligned} \tag{19}$$

where h is the parametric element length.

3 Experimental Results

The new 3-D registration method using the deformable surface-spine model has been applied to matching surgical prostates for statistical modeling of localized prostate cancer. 3-D computerized prostate models have been reconstructed using deformable surface-spine models resulting in a great consistency in nonlinear interpolation and accurate surface shape representations. Fig. 3 demonstrates how the initial model responds to external forces defined by the goal contours and gradually fit to the contours. An example of the reconstructed prostate model is shown in Fig. 4, which includes all the anatomical structures of interest such as the prostate capsule, urethra, seminal vesicles, ejaculatory ducts and the different carcinomas. We then apply our deformable surface-spine model to registering computerized prostate models for computing the nonlinear deformations encountered in matching two complex-structured prostate models. The initial two surgical prostate models to be matched are shown in Fig. 5(a), and the two matched prostates are displayed in Fig. 5(b).

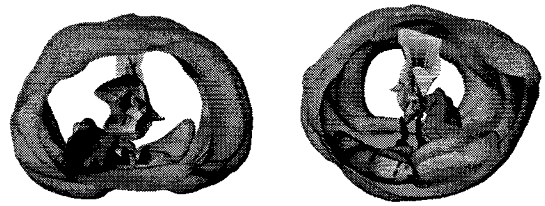

(a) (b)

Figure 4: A reconstructed prostate model: (a) the front view, (b) the rear view.

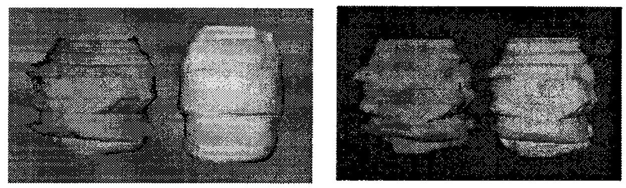

(a) (b)

Figure 5: Matching two prostates: (a) before matching, (b) after matching.

4 Conclusion

In this paper, we have developed a new 3-D registration method based on a finite-element deformable surface-spine model. The method has been applied to registration of computerized surgical prostate models for statistically modeling the disease pattern of localized prostate cancer. Experimental results have demonstrated that the new 3-D registration method can successfully match complex-structured surfaces by recovering nonlinear deformations from the dynamic property of the deformable surface-spine model.

References

[1] N. Ayache, "Medical Computer Vision, Virtual Reality and Robotics," *Image and Vision Computing,* vol. 13, no. 4, pp. 295-311, May 1995.

[2] G. Celniker and D. Gossard, "Deformable Curve and Surface Finite-Elements for Free-Form Shape Design," *Computer Graphics*, vol. 25, no. 4, pp. 257-266, July 1991.

[3] M. Moshfeghi, S. Ranganath, and K. Nawyn, "Three-Dimensional Elastic Matching of Volumes," *IEEE Trans. on Image Processing,* vol. 3, no. 2, pp. 128-138, Mar. 1994.

[4] D. Terzopoulos, A. Witkins and M. Kass, "Constraints on Deformable Models: Recovering 3D Shape and Non-rigid Motion," *Artificial Intelligence,* vol. 36, pp. 91-123, 1988.

[5] Zienkiewicz, *The Finite Element Method,* The Third Edition, McGraw-Hill Book, 1967.